# Optimisation of Resistive Wall Mode Control in STEP

Guoliang Xia[1], T.C. Hender[1], Yueqiang Liu[2] and E. Trier[1]

[1]UKAEA, Culham Science Centre, Abingdon, OX14 3DB, United Kingdom of Great Britain and Northern Ireland

[2]General Atomics, PO Box 85608, San Diego, CA 92186-5608, United States of America

E-mail of corresponding author Guoliang.Xia@ukaea.uk

## 1. Introduction

The Spherical Tokamak for Energy Production (STEP) is a UKAEA program that aims to deliver a prototype fusion energy plant and a path to commercial viability of fusion [1]. The low aspect ratio spherical tokamak is attractive because of its potential to achieve high beta β operation, and fusion power ~ $\beta^2$. To fully exploit this, and to maximize economic attractiveness, operation above the no-wall β-limit is desirable, where the resistive wall mode (RWM) must be controlled either by passive or active control, since otherwise this may lead to major disruption.

Understanding and controlling the RWM is a key issue for the optimisation of plasma pressure and improving the economic benefit. Previously, it was found that passive stabilization of the RWM in STEP gives a relatively small increase in $\beta_N$ above the no-wall limit, relying on toroidal plasma flow and drift kinetic resonance damping (from both thermal and energetic particles) [2]. In order to optimise performance in STEP from an MHD viewpoint, active control of the unstable RWM appears to be a necessity. In this work, the MARS-F code [3] is utilized to model feedback schemes for controlling the $n$=1 RWM in STEP, assuming a set of active coils located near the outboard mid-plane of the torus.

## 2. Equilibrium and plasma flow effect

The equilibrium studied is a case of plasma current $I_p$=21 MA, the major radius $R_0$=3.64 m, $B_0$=2.3 T is the toroidal magnetic field at the plasma centre. The case studied has an aspect ratio $A$=1.67. The safety factor has values of $q_0$=2.15 on the magnetic axis, $q_{min}$=2.09, and $q_e$=9.86 at the plasma edge, the target plasma has the normalized beta value of $\beta_N$=5.2. Fig. 1 shows the radial profiles for some key equilibrium quantities.

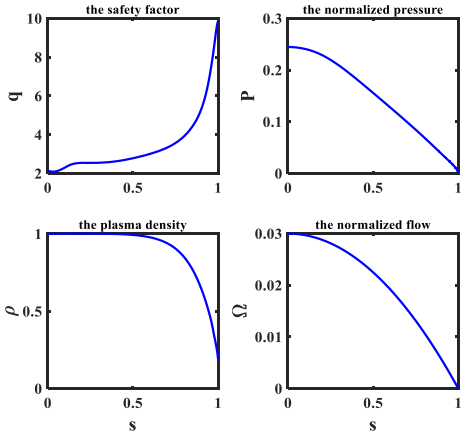


Fig. 1: The safety factor, plasma pressure, density, and toroidal flow profiles versus the magnetic surface label $s$ (the square root of the normalized poloidal flux).

The STEP design continues to evolve and the case shown is a particular example. The results presented do cover the effect of reduced beta as an option. The MARS-F computed no-wall beta

limit is $\beta_N^{no-wall} = 4.37$, and the ideal-wall (conformal wall) beta limit is $\beta_N^{ideal-wall} = 6.39$. For the target plasma, the plasma flow cannot stabilize the RWM, feedback control appears to be a necessity.

## 3. Feedback control with flux-to-current scheme

In the flux-to-current control scheme, the measured flux from the RWM is used to control the current in the feedback coils, which are assumed to be mid-plane coils at *R*=7.15 m in this case. Figure 2 shows the Nyquist plots with radial sensor and poloidal sensor which simulated with a proportional (P) controller. With the flux-to-current control scheme, the feedback control is achieved with P controller only. The poloidal sensor (counter-clockwise encircles) is more robust than the radial sensor, following the Cauchy principle of phase variation.

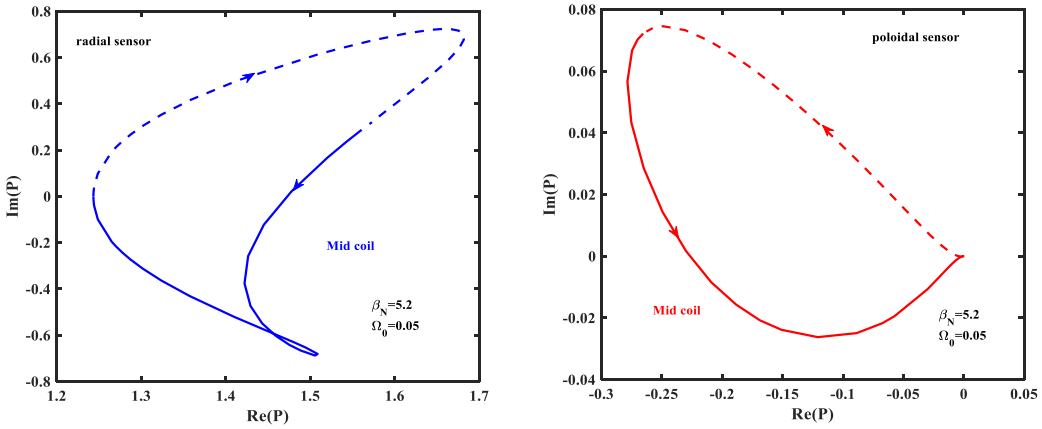


Fig. 2: Nyquist plots with radial sensor (Left) and poloidal sensor (Right)

An alternative approach of investigating the critical feedback gain value to suppress the RWM is to compute the plasma response to applied currents in active coil transfer function in the presence of plasma flow. The plasma response approach and the direct feedback approach simulated with MARS-F recovers the same critical gain value as shown in Fig. 3. An optimal gain phase of the mid-plane active coil can minimize the critical gain value.

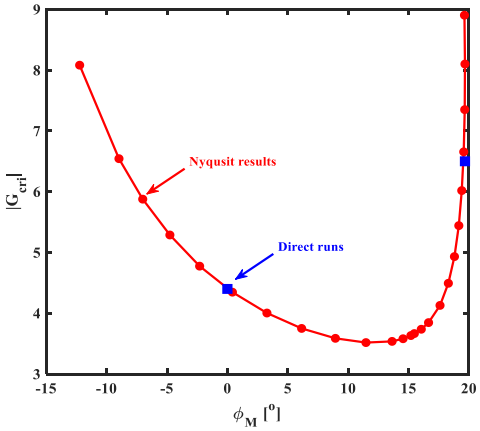


Fig. 3: The critical feedback gain value versus the gain phase of the mid-plane active coil

The disadvantages of flux-to-current control scheme are (i) the current in the active coils is eventually driven by the power supply voltage, and (ii) the flux-to-current scheme does not allow flexibility compared with the flux-to-voltage logic (next section), i.e. as soon as the current limit is reached, the RWM control is lost [4].

## 4. Feedback control with flux-to-voltage scheme

Equation (1) represents the flux-to-voltage control scheme, which is the basic choice. It should be noted with this scheme, even in the absence of feedback control, the active coils do provide a weak passive stabilizing effect of ~10% on the RWM growth rate. The same control logic has been assumed in previous RWM control studies for ITER [5]. While simulations show that a P controller alone ($K_d$=0) does not yield complete stabilization of the mode even considering 5% of the Alfven speed (Fig. 4). The abrupt change of the eigenvalue behavior at certain feedback gain value is due to the merging of two branches of closed-loop solutions into a complex conjugate pair, resulting in a RWM instability that weakly depends on the feedback gain. As a result, a weakly unstable residual (and rotating) closed-loop RWM remains with P controller alone, even at large feedback gain.

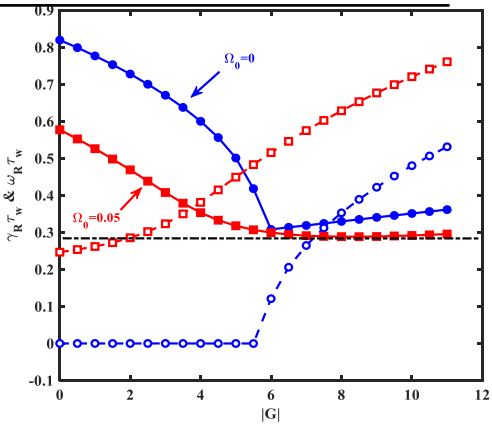


Fig. 4: The computed eigenvalue versus the feedback gain. The closed symbols indicate the growth rate and the open symbols the mode frequency. (This applies to all following figures)

$$\frac{d\psi_f}{dt} + R_f I_f = V_f = -G\left(K_p + K_d \tau_f \frac{d}{dt}\right) b_s \qquad (1)$$

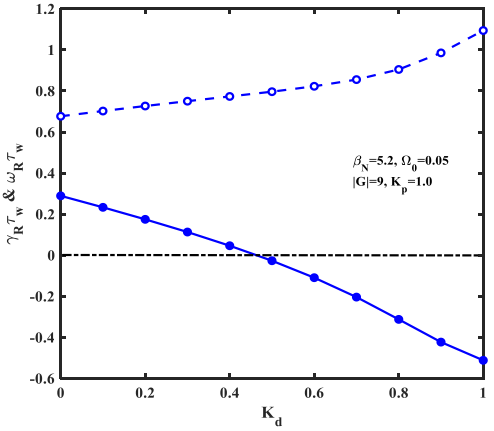


Fig. 5: The MARS-F computed eigenvalue of the $n$ = 1 RWM versus the derivative gain factor

Adding a modest derivative action ($K_d$=0.5) in Eq. (1), i.e. an ideal proportional and derivative (PD) controller, and assuming an ideal situation without any noise in the closed loop, the RWM in STEP can be fully stabilized in the presence of plasma flow as shown in Fig 5. Simulated with a PD controller, the critical feedback gain value decreases with increasing the derivative gain factor $K_d$ (Fig. 6), but the disadvantage of high derivative gain is that it accentuates the effect of noise on the sensor signal, as discussed in the next section.

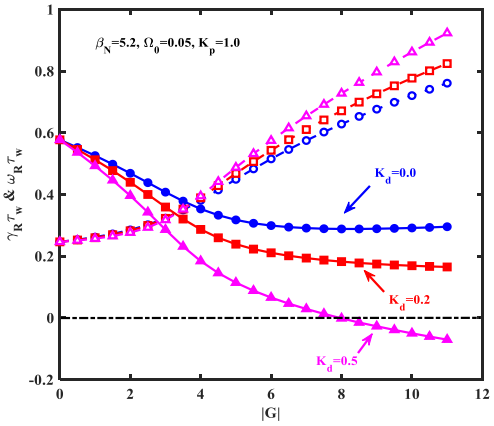


Fig. 6: The computed eigenvalue versus the feedback

## 5. Effect of sensor noise with PD controller

A key aspect in the performance of feedback controller is the presence of noise in the detected signal(s) [6]. In the present study, random numbers with a normal distribution, zero mean and standard deviation of $\sigma_{noise}$=0.1 G, are injected into the perturbed magnetic field sensor signal,

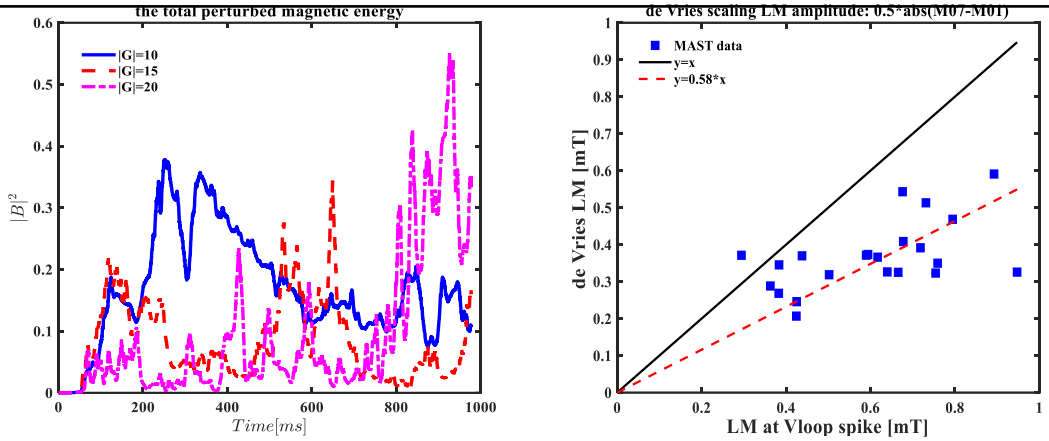


Fig. 7: Two criteria are proposed to judge the control loop success

when the closed-loop system is modelled with the initial value approach. With more realistic control assumptions, the RWM feedback is found to be of a more subtle issue in STEP. This is partially due to the fact that the derivative action tends to amplify the sensor noise, and partially related to the statistical nature of the problem leading to difficulties. Two criteria are proposed to judge the control loop success (Fig. 7). One is based on the total perturbed magnetic energy of the system; another is via assessing whether the control is sufficient to avoid disruption [7]. To obtain reliable results, 100 initial value closed-loop simulations are performed for the same feedback configuration, with statistics drawn in terms of the success rate for the RWM suppression. Figure 8 shows success rates of feedback control with sensor noise exceeding 90% are achieved, and generally increase with the proportional feedback gain. Neither the average, nor the maximum sensor amplitude calculated by MARS-F, reach the predicted disruptive amplitude, i.e. 37G, meaning the RWM is very unlikely to lead to a disruption for the modelled feedback control (Fig. 9).

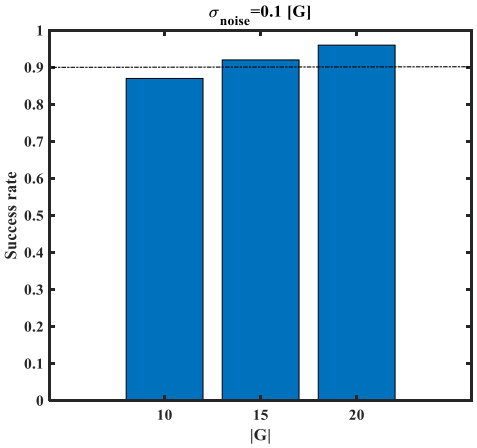


Fig. 8: Success rate versus the feedback gain

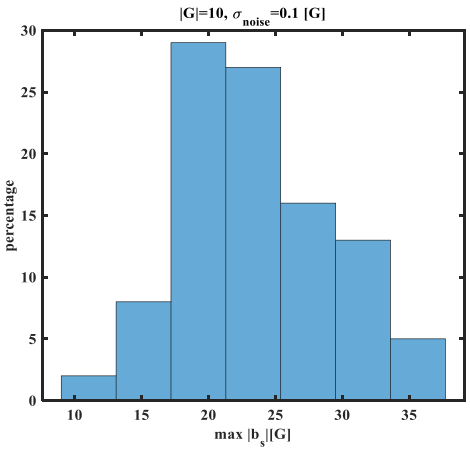


Fig. 9: The percentage of maximum sensor amplitude over the 100 simulations for gain value |G|=10 between 0.1 and 1 s

## Reference

[1] Wilson H R et al 2020 Commercialising Fusion Energy 2053 8-18
[2] http://ocs.ciemat.es/eps2021pap/pdf/P1.1042.pdf
[3] Liu Y Q et al 2000 Phys. Plasmas 7 3681
[4] Li L et al 2012 Phys. Plasmas 19 012502
[5] Wang S. et al 2019 Nucl. Fusion 59 096021
[6] Liu Y Q et al 2016 Fusion Science and Technology 70 387-405
[7] de Vries P C et al 2016 Nucl. Fusion 56 026007